World Academy of Science, Engineering and Technology
International Journal of Mechanical and Mechatronics Engineering
Vol:6, No:12, 2012

Generating High-Accuracy Tool Path for 5-axis Flank Milling of Globoidal Spatial Cam

Li Chen, ZhouLong Li, Qing-zhen Bi and LiMin Zhu

Abstract—A new tool path planning method for 5-axis flank milling of a globoidal indexing cam is developed in this paper. The globoidal indexing cam is a practical transmission mechanism due to its high transmission speed, accuracy and dynamic performance. Machining the cam profile is a complex and precise task. The profile surface of the globoidal cam is generated by the conjugate contact motion of the roller. The generated complex profile surface is usually machined by 5-axis point-milling method. The point-milling method is time-consuming compared with flank milling. The tool path for 5-axis flank milling of globoidal cam is developed to improve the cutting efficiency. The flank milling tool path is globally optimized according to the minimum zone criterion, and high accuracy is guaranteed. The computational example and cutting simulation finally validate the developed method.

Keywords—Globoidal cam, flank milling, LSQR, MINIMAX.

I. Introduction

GLOBOIDAL spatial cam is an intermittent transmission mechanism with roller follower turrets. It has been widely used in chip mounting devices, packing machines and assembly lines, as well as machine tool and pallet changers [15]. Compared with traditional intermittent transmission mechanism, the globoidal indexing cam mechanism has advantages on transmission speed, dynamic performance, indexing accuracy, carrying capacity and reliability. The cam profile surface is usually generated by the conjugate contact motion of the roller. The obtained sculptured surface is complex to machine. Conventional methods of cam production are time-consuming and error-prone. The 5-axis machine tool provides a powerful method to machine spatial cam software. However, the commercial CAM software cannot generate NC program for the globoidal spatial cam, which must be designed by incorporating the transmission mechanism.

Three methods can be used to machine the meshing profile surfaceas shown in Fig.1.

(1) Equivalent processing [15]. The profile surfaces are machined by the cylindrical cutter whose diameter is the same as the rollers. The cutter' motion is identical to the roller's motion. In theory, there is no deviation between the profile surface and the cutter's envelop surface. Usually expensive customizing tools are used to fit the roller's diameter. The other shortcoming of the method is that the machined surface quality is difficult to achieve. Both sides of the cutter will remove materials simultaneously in the finishing machining. The cutter's vibration and distortion are hard to avoid in the cutting conditions.

Prof. Zhu, Mr. Chen, Mr. Li and Dr. Bi are with State Key Laboratory of Mechanical System and Vibration, Shanghai Jiao Tong University, Shanghai, 200240, PR China(LiMin Zhu e-mail: zhulm@sjtu.edu.cn).

Manuscript received July 30, 2012; Accepted October 15, 2012.

(2) 5-axis point-milling. The profile surface is machined by using a 5-axis machine tool with a ball-end cutter or flat-end cutter. R-S Lee and J-N Lee have presented a detail tool path planning method using point-milling [10], [11], [12]. The tool path of the point milling includes tool contact point and tool axis vector. The tool contact point is sampled from the cam profile surface, while tool axis vector is calculated according to the contact angle of the contact point. The 5-axis point-milling method provides a simple way to machine the profile surface by using the general machine tool. However, the point-milling method is time-consuming, and the machined surface has cusp height.

(3) 5-axis flank milling [16]. Flank milling is a line-contact machining method. Compared with the point-milling method, flank milling can achieve smoother surface finish with significant efficiency improvement. Generating tool path for flank milling of the globoidal indexing cam is challenging because the cam profile is a complex surface. Usually a deviation exists between the profile surface and the tool envelope surface. The difficulty of the tool path generation is to minimize the deviation to acceptable levels. The problem of optimum positioning of a cylindrical cutter has been studied extensively [2-8]. Many tool path generation algorithms have been proposed to machine the ruled surface, but the cam profile surface is not ruled surface. Existing general-purpose algorithm cannot generate the tool path for flank milling of the globoidal indexing cam.

We propose a new tool path planning method for 5-axis flank milling of a globoidal indexing cam. The cam profile surface is computed by the homogeneous coordinate transformation and conjugate surface theory. The discrete tool position is first optimized based on the instantaneous contact curve, and the flank milling tool path is finally globally optimized according to the minimum zone criterion.

The remainder of the paper is organized as follows.Section II introduces the geometry of the globoidal indexing cam mechanism and gives the instantaneous contact curve. In Section III, the discrete tool position is first generated, and the tool path is the globally optimized. Section IV illustrates a computational example to validate the developed method.

II. Globoidal indexing cam mechanism

Fig.2 shows the geometry of a globoidal indexing cam mechanism. The mechanism consists of three parts: the turret, the rollers and the globoidal cam. The globoidal cam is the driving part of the mechanism; it rotates around the input axis. When the cam rotates, the indexing profile surface pushes the

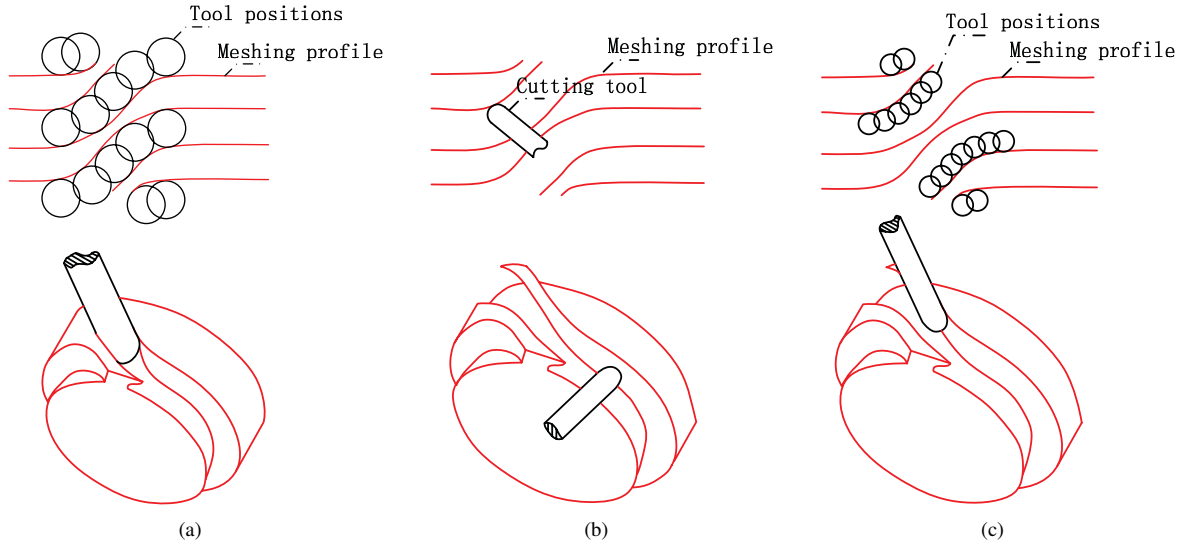

Fig. 1. (a) Equivalent processing, (b) 5-axis point-milling, (c) 5-axis flank milling

rollers to orbit the rotation axis of the turret, e.g. the output axis shown in figure 1. In this paper, the profile surface of the cam is generated by roller's motion, as a consequence, the spatial cam's meshing profile surface and rollers' cylindrical boundary surfaces are in conjugate contact motion, thus satisfy the constraints as follows[14]:

1. Contact points must coincide on the conjugate surface, respectively;

2. Conjugate surfaces have a common normal at the contact point;

3. Component of relative velocity at the contact points is equal to zero along the common normal.

We need to establish a series of coordinate systems to simplify the calculating process to solve the expression of the cam's profile surface. $(OXYZ)_0$ and $(OXYZ)_0{}'$ are the coordinate systems for the fixed frame; $(OXYZ)_c$ is the coordinate system attached to the cam; $(OXYZ)_t$ is the coordinate system for the turret; $(OXYZ)_{r_i}$ is the coordinate system attached to the i-th roller.

The expression of the roller's cylindrical surface under $(OXYZ)_t$ is as follow:

$$\begin{bmatrix} x_t \\ y_t \\ z_t \end{bmatrix} = \begin{bmatrix} r \\ R_r \cos\psi \\ R_r \sin\psi \end{bmatrix}, r \in [R_t, R_t + h_r], \psi \in [0, 2\pi] \quad (1)$$

R_r is the radius of roller, R_t is the radius of the turret, h_r is the height of rollers. The expression of the conjugate contact curve is as follow:

$$\tan\psi = \frac{pr}{C - r\cos\phi}\left(\frac{\omega_t}{\omega_c}\right) \quad (2)$$

ω_t and ω_c are the angular velocities of turret and cam respectively.

ϕ stands for the spatial position of the roller. ω_t and ω_c are the angular velocities of turret and cam respectively. The expression of the profile surface under $(OXYZ)_c$ is as follow:

$$\begin{bmatrix} x_c \\ y_c \\ z_c \end{bmatrix} = \begin{bmatrix} x_t\cos\phi\cos\theta - py_t r\sin\phi\cos\theta - z_t\sin\theta - C\cos\theta \\ -x_t\cos\phi\cos\theta - py_t r\sin\phi\cos\theta - z_t\sin\theta + C\cos\theta \\ px_t\sin\phi + y_t\cos\phi \end{bmatrix} \quad (3)$$

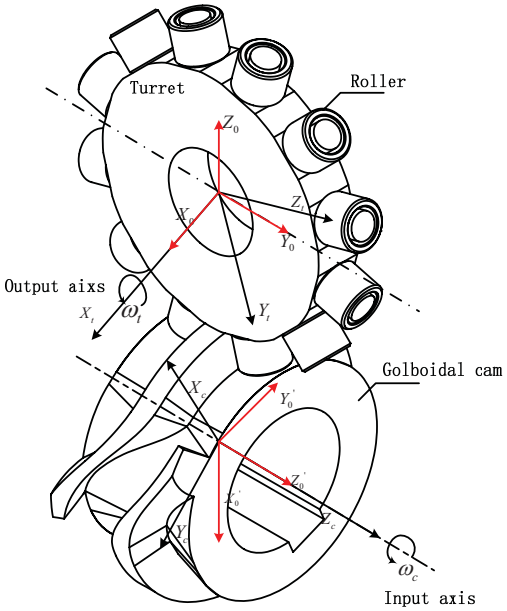

Fig. 2. Geometry of globoidal cam mechanism

θ is cam's rotation angle, p is cam's rotation factor, when cam rotates counterclockwise, p = -1, when cam rotates clockwise, p = 1.

For convenience, we use homogeneous transformation to evaluate the profile surface's expression. It only takes one matrix to completely describe a translation or a rotation or a combination in a Cartesian coordinate system by homogeneous transformation; equivalently, a matrix can also completely describe a transformation form one Cartesian coordinate system to another.

A roller's axis under $(OXYZ)_0$ can be expressed as fol-

lows:

$$\begin{bmatrix} x_0 \\ y_0 \\ z_0 \end{bmatrix} = \begin{bmatrix} R_t \cos\phi \\ R_t \sin\phi \\ 0 \end{bmatrix} \quad (4)$$

ϕ is the rotation angle of the turret. Express (4) in a four-dimensional-vector form in order to apply homogeneous transformation:

$$A_0 = [R_t \cos\phi, R_t \sin\phi, 0, 1]^T \quad (5)$$

According to homogeneous transformation, the transform from coordinate system $(OXYZ)_0$ to $(OXYZ)_0{}'$ and coordinate system $(OXYZ)_0{}'$ to $(OXYZ)_c$ can be expressed as:

$$T_{00'} = \begin{bmatrix} 1 & 0 & 0 & -C \\ 0 & 1 & -1 & 0 \\ 0 & 1 & 0 & 0 \\ 0 & 0 & 0 & 1 \end{bmatrix}, T_{0'c} = \begin{bmatrix} \cos\theta & \sin\theta & 0 & 0 \\ -\sin\theta & \cos\theta & 0 & 0 \\ 0 & 0 & 1 & 0 \\ 0 & 0 & 0 & 1 \end{bmatrix} \quad (6)$$

C is distance from turret's center to the spatial cam's center. Than the roller's axis's expression under the coordinate system $(OXYZ)_c$ can be obtained:

$$A_c = T_{0'c} T_{00'} A_0 = \begin{bmatrix} r\cos\theta\cos\phi - C\cos\theta \\ -r\sin\theta\cos\phi + C\sin\theta \\ r\sin\phi \\ 1 \end{bmatrix} \quad (7)$$

Therefore, the axial trajectory surface of the roller under the coordinate system $(OXYZ)_c$ is:

$$\begin{bmatrix} x_c \\ y_c \\ z_c \end{bmatrix} = \begin{bmatrix} r\cos\theta\cos\phi - C\cos\theta \\ -r\sin\theta\cos\phi + C\sin\theta \\ pr\sin\phi \end{bmatrix} \quad (8)$$

We yet to obtain the meshing profile surface of cam. As mentioned earlier, the profile surface of the cam is the axial trajectory surface of the roller offset by a distance of R_r :

$$S_p(u,v) = S_r(u,v) + R_r n(u,v) \quad (9)$$

$n(u,v)$ is the unit normal vector at the (u, v) point. Currently there is no ideal algorithm to generate the offset surface's analytical expression. A computational approach is to discretize the generant according to accuracy requirements, and offset the points by their local normal vectors, finally, use a surface to fit the point cloud. In this application or many other circumstances, the point cloud is sufficed, consequently the last step can be skipped.

The normal vector at a position in the axial trajectory surface of the roller can be easily obtained, since the analytical expression of the surface has been solved:

$$N(u,v) = N(r,t) = [\frac{p\sin\phi\sin\theta(r\cos\phi - C)\omega_c + pr\cos\theta\omega_t}{\cos\phi(r\cos\phi - C)\omega_c}, \frac{p\sin\phi\sin\theta(r\cos\phi - C)\omega_c - r\sin\theta\omega_t}{-\cos\phi(-r\cos\phi + C)\omega_c}, -1] \quad (10)$$

Unitized $N(u,v)$ will we obtain $n(u,v)$ we desire. To avoid computational complications, error diffusions caused by the analytical solution and above all, to make our algorithm robust, a numerical algorithm is chosen to solve the unit normal vector:

Algorithm1:

(1). Solve the derivatives on the two parameter curves at the given points(differentials instead of derivatives in practical situations should be used);

(2). Solve the cross product of the two vectors obtained in step(1) as the normal vector;

(3). Unitized the normal vector.

III. Processing program

The main process of the approximation tool path planning can be described as follows:

1. Find a set of discrete tool positions as an initial solution;
2. Fit these rulings with a ruled surface;
3. Use optimizing strategies to minimize the error.

The rest part of this chapter will describe these steps in details.

1. Find a set of discrete tool positions as an initial solution:

In the existing tool position compensate methods, initial solution is obtained by middle point offset algorithm or two point offset algorithm[2]. The tool positions obtained in this way tend to have large error. To obtain a more satisfactory initial solution, here we consider a more accurate approach:

As mentioned above, the axial trajectory surface of the roller is a ruled surface which is not developable during the indexing period. By the definition of undevelopable ruled surface, along a specific ruling, normal unit vectors are not equal. Therefore the mapping for a ruling on the offset surface is a spatial curve -shown in Fig 3.

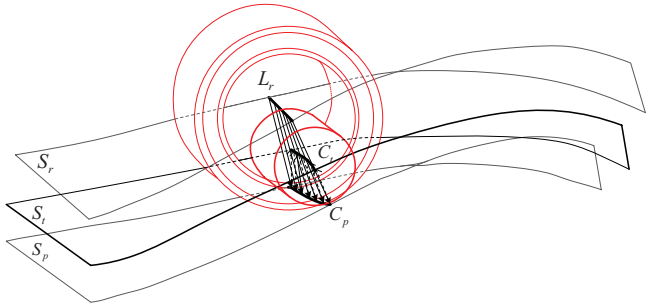

Fig. 3. Initial solution for tool axial trajectory

S_r is the axial trajectory surface of the roller, S_p is the S_r's offset surface by the distance of the radius of the roller, namely the meshing profile surface of the cam; L_r is one specific ruling on S_r , which corresponds to a specific roller position; C_p is the mapping of L_r on S_p - the profile surface of the cam. Now conduct the same processes, we obtain C_t, which is the mapping of C_p on S_t - the theoretical tool axial trajectory surface.

Repeat the processes and find a set of discrete ruling on S_r and a set of spatial curves on S_t . Usually, if the ruled surface S_r is not too "distorted" - the unit normal vectors change in a small scope along one ruling - the spatial curves corresponding to the discrete rulings have relatively small curvatures and big curvature radiuses at most positions, that means any curve from the set we obtain, would not "wonder" too far from a hypothetical straight line. So if those curves are fitted with a set of straight line segments, a set of discrete rulings with

sustainable errors will be obtained as initial solution of the problem.

Here we consider a computational approach, and treat a spatial curve as a discrete set of special points; those points can be approximated by a line segment.

Algorithm2 (Fig.4):

(1). Sample a set of points R_n spatially evenly on L_r of the roller axial trajectory surface;

(2). Apply Algorithm1 to obtain a set of unit normal vectors of S_r at R_n, and offset R_n by the radius of the rollers along the unit normal vectors, we get another set of points P_n, which by definition, are on the meshing profile surface of spatial cam;

(3). Apply Algorithm1 to obtain a set of unit normal vectors of S_p at P_n, and offset P_n by the radius of the cutter along the unit normal vectors, we get another set of points T_n, which by definition, are on the theoretical tool axial trajectory surface;

(4). Fit T_n with a line segment L_t in a least square sense.

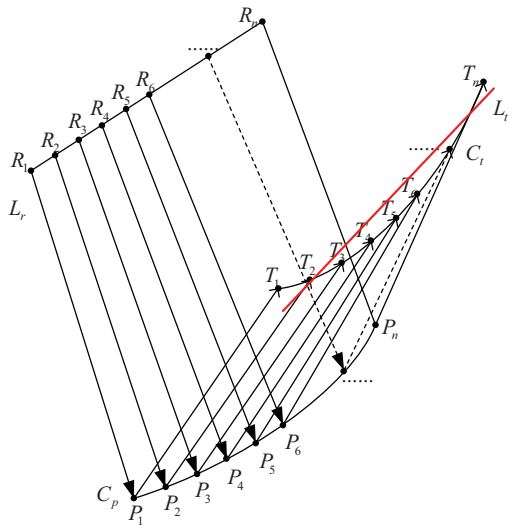

Fig. 4. Find initial solution

2. Fit these rulings with a ruled surface:

The result of the first step is a set of discrete rulings; the task of this step is to find a ruled surface to fit these rulings in sequel. A ruled surface can be treated as a trajectory of a straight line, subsequently a ruled surface can be expressed in the following form:

$$S_{RL}(u,\theta) = [I + \frac{\hat{\omega}}{\|\omega\|}\sin(\|\omega\|\,\theta) + \frac{\hat{\omega}^2}{\|\omega\|^2}(1-\cos(\|\omega\|\,\theta))]$$
$$(tp+(1-t)q) + [\frac{\hat{\omega}}{\|\omega\|}\sin(\|\omega\|\,\theta) +$$
$$\frac{\hat{\omega}^2}{\|\omega\|^2}(1-\cos(\|\omega\|\,\theta))]b + h\theta\omega, t\in[0,1], \theta\in[0,\theta_{u_f}] \quad (11)$$

p and q are the two end points of the line segments.

A ruled surface can also be regarded as a result of conjoining corresponding points on the two spatial curves with straight line segments, thus a ruled surface can be expressed in the following form:

$$S(u,v) = v\cdot c_1(u) + (1-v)\cdot c_2(u), v\in[0,1] \quad (12)$$

$c_1(u)$ and $c_2(u)$ are the two directrices of the surface. In this paper, the later form is preferred. The surface (11) represents has the same line segments length at any parameter position of the directrix, thus the boundaries' properties may not be satisfactory in practical situations, adaption procedures are complicated and robustness are weakened. Moreover, the optimization process afterwards mostly focuses on control points of the directrices. So in this paper, the later form is preferred.

Algorithm 3: find the ruled surface's two directrices c^{top} and c^{bot}

(1). Treat the line segments generated in algorithm 2 as two groups of points: ${I^{top}}_n$ - starting points, ${I^{bot}}_n$ - ending pointsand treat them as two groups of B-spline interpolation points;

(2). Reverse control points ${C^{top}}_m$ and ${C^{bot}}_m$ according to the interpolation points ${I^{top}}_n$ and ${I^{bot}}_n$ respectively;

(3). In order to fit the line segments with the ruled surface, the parameter u at ${I^{top}}_i$ on c^{top} and ${I^{top}}_i$ on c^{bot} should be equal. Therefore the knot vectors for the construction of two cubic B-spline curves c^{top} and c^{bot} should be the same. In this paper, cumulative chord length is used as measure to determine the knot vectors K_{n+4}. If the chord length here is simply defined as the Euclidean distance between two points, based on experience, the ruled surface would be undesirably uneven. Here chord length as the distance of two line segments in Euclidean space is defined according to [1]. Definition 1: The distance of two line segments $l_1(p_1,q_1)$ and $l_2(p_2,q_2)$ in Euclidean space

$$d(l_1,l_2)^2 := 3\int_0^1[(1-\lambda)(p_1-p_2)+\lambda)(q_1-q_2)]^2 d\lambda$$
$$= [(p_1-p_2)^2 + (q_1-q_2)^2 + (p_1-p_2)\cdot(q_1-q_2)] \quad (13)$$

(4). Construct two cubic B-spline curve c^{top} and c^{bot} by control points ${C^{top}}_m$, ${C^{bot}}_m$ and common knot vectors K_{n+4}. Now that the two directrices c^{top} and c^{bot} are decided, the ruled surface's expression is obtained:

$$S(u,v) = v\cdot c^{top}(u) + (1-v)\cdot c^{bot}(u) \quad (14)$$

3. Use optimizing strategies to minimize the error.

The present researches regarding the tool position optimizing problem mostly treat the tool position individually, thus to process one tool position at a time. The optimizing problem then transforms to minimize the distance from a line segment to a spatial surface. Bedi's work [7], Li et al. [9] presented a three-step-optimization approach, which needs to solve three transcendental equations numerically. The program is easy to implement and fast to compute. This method overlooks the fact that the milling is a continuous process time and space, treating each tool position individually would undermine the integrity of the process, subsequently creating a negative impact on the smoothness and accuracy of the process. As shown in Fig5, C_u is a special curve served to determine one cutter location, the theoretical optimal solution is L_u, which is a line segment best fit C_u, while we treat the process as a whole - the tool axial trajectory S, it can be easily discovered that there is an obviously better solution L_s, which lies on the axial trajectory surface completely.

On the other hand, many researchers have considered another alternative: serve the overall error as the optimization goal.

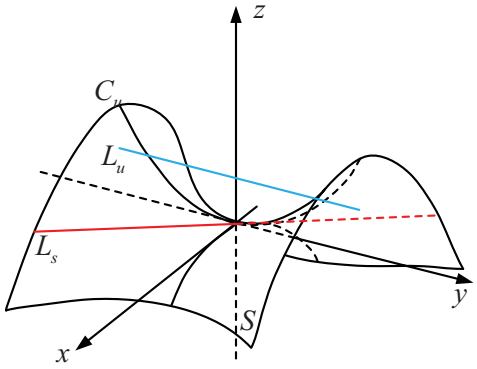

Fig. 5. Comparison of local optimization and global optimization

In this paper, the overall error means the distance of two surfaces -the theoretical tool axial trajectory surface and the ruled surface, for the ruled surface, an initial solution is obtained in step one.

According to ANSI and ISO standard, serve S_1 as datum surface, the error between the two surfaces can be defined as:

Definition 2:

$$e_1 = \max_{p \in s_2} d_{p,s_1} \tag{15}$$

d_{p,s_1} stands for distance from a point to a surface, which is defined as follow:

Definition 3:

P is a point in euclidean-3 space; there exist at least one point Q on the surface S satisfies

$$\|P - Q\| = \min_{X \in S} \|P - X\| \tag{16}$$

The distance from the point P to the surface S is:

$$d_{p,s} = \|P - Q\| \tag{17}$$

As can be seen from the definition 2, it is difficult to calculate the distance between two surfaces. In order to achieve a computational and universal approach, we consider discretizing the target surface, in this case, the theoretical tool axial trajectory surface, into a set of point cloud, and serve a set of point-surface errors as the optimization target.

According to the definition of B-spline curve, the ruled surface's directrices c^{top} and c^{bot} obtained in the step 2 can be expressed as:

$$c^{top}(u) = \sum_{i=0}^{m} N_{i,k} {C_i}^{top}, c^{bot}(u) = \sum_{i=0}^{m} N_{i,k} {C_i}^{bot} \tag{18}$$

Submit 18 to 14, it can be discovered that the control points of the two directrices determine the ruled surface completely. Naturally, the control-points' coordinate-matrix expressed in 19 will be served as optimization control variables.

$$w^T = [C_0^{top}, ..., C_m^{top}, C_0^{bot}, ..., C_m^{bot}]^T \tag{19}$$

Consider a least-squares sense approach, the optimizing problem become as follows:

$$\min_{w} \sum_{i=1}^{n_{cloud}} \left(d^{S_t}_{P_i,S_{ruled}(w)}\right)^2 \tag{20}$$

According to definition 3, $d^{S_t}_{P_i,S_{ruled}(w)}$ has no analytical expression, but Zhu and Zheng [3] have proved that the ordinary gradient and the Heather matrix can be solved:

$$d^{S_t}_{P_i,S_{ruled}(w)}(P + \Delta P, w + \Delta w) = d^{S_t}_{P_i,S_{ruled}(w)}(P, w) + n^q \cdot \Delta P - [n^q \cdot \psi_{w_1}, ..., n^q \cdot \psi_{w_l}]^T \cdot \Delta w \tag{21}$$

$$\begin{aligned}[\nabla^2 d(w)]_{ij} = {} & [\psi_u \cdot \psi_{w_i}, \psi_v \cdot \psi_{w_i}] G^{-1} \Omega A^{-1} [\psi_u \cdot \psi_{w_j}, \psi_v \cdot \psi_{w_j}]^T \\ & - d(w) [\psi_u \cdot \psi_{w_i}, \psi_v \cdot \psi_{w_i}] G^{-1} \Omega A^{-1} [n^q \cdot \psi_{uw_j}, n^q \cdot \psi_{vw_j}]^T \\ & - n^q_{w_j} \cdot \psi_{w_i} \\ & - [n^q \cdot \psi_{w_i u}, n^q \cdot \psi_{w_i v}] A^{-1} [\psi_u \cdot \psi_{w_j}, \psi_v \cdot \psi_{w_j}]^T \\ & + d(w) [n^q \cdot \psi_{w_i u}, n^q \cdot \psi_{w_i v}] A^{-1} [n^q \cdot \psi_{uw_j}, n^q \cdot \psi_{vw_j}]^T - n^q \cdot \psi_{w_i w_j}\end{aligned} \tag{22}$$

Then the problem can be solved by common methods like the Gauss-Newton method.

In practical process, maximum error takes more concern; accordingly a minimax approach can lead to a more satisfying result. The optimizing problem can be described as follows:

$$\min_{w} \max_{1 \le i \le n_{cloud}} \left| d^{S_t}_{P_i,S_{ruled}(w)} \right| \tag{23}$$

This is a typical sequential linear programming (SLP) problem; many concise and efficient algorithms are introduced to solve this problem, such as interior point method and simplex method.

Based on experience, algorithms for SLP problems always require an initial solution with relatively high quality. Otherwise, the programming would require larger step size for iterations, thus the programming wouldn't have a very satisfactory convergence and the accuracy would be undermined.

Luckily, the G-N method in the least-square sense mentioned above has a very good convergence regardless the quality of the initial solution and the complexity of the algorithm is low, thus the computation time is very short. Consequently in practical situations, a feasible approach is to process the initial solution we get form the step two with least-square method, and use the result as initial solution for the SLP process.

The entire process is shown in Fig6:

IV. Example

TABLE I
PARAMETERS CHOSEN FOR THE GLOBOIDAL INDEXING CAM MECHANISM

The speed of the cam n_c	300r/min
The angular velocity of the cam	$2\pi n_c/60 = 10\pi$
Rotation angel during the indexing period	$\theta_h = 72°$
Rotation angel during the resting period	$\theta_t = 2\pi - \theta_h = 288°$
The direction of rotation of the cam P	P=-1
Number of the cam's heads	H=1
The sub-degree of the turret	I=12
The number of the rollers	Z=HI=12
The rotation angle of turret during the indexing period	$\theta_d = 2\pi/I = \pi/6$
Modified sinusoidal acceleration	$\theta_d = 2\pi/I = \pi/6$
The diameter of rollers D_r	14mm
The center distance C	80mm
The radius of the spatial cam R_c	40
The radius of the pitch circle of the turret R_t	40mm
The height of the roller h_r	12mm

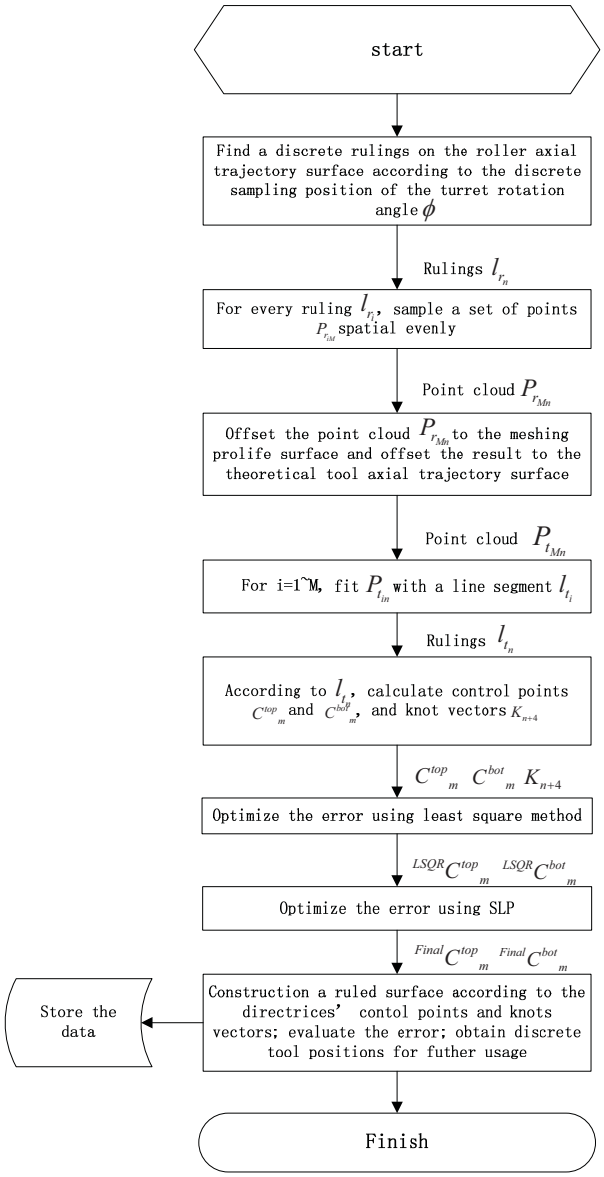

Fig. 6. The tool path generation porcess.

With the Parameters given in Table1, a globoidal indexing cam mechanism is uniquely determined, as shown in Fig7:

We select a cylindrical tool with a 3mm radius to process the meshing profile Algorithm 2 offers us an optimal solution in a single-tool-position-oriented sense. The error distribution on the theoretical tool trajectory surface is shown in Fig8:

Using the LSQR method described in chapter 3, we obtain a tool trajectory. Fig9 shows the error distribution on the theoretical tool trajectory surface:

As can be seen, in most areas of the surface, the error is considerably small (under 1). Error above 3only occur in very small scales. This phenomenon fits the nature of the LSQR method's optimizing goal described in (14), which is the overall error.

As can be seen, after LSQR is applied, the overall error has been reduced to a level fewer than 10 micorns, which meets

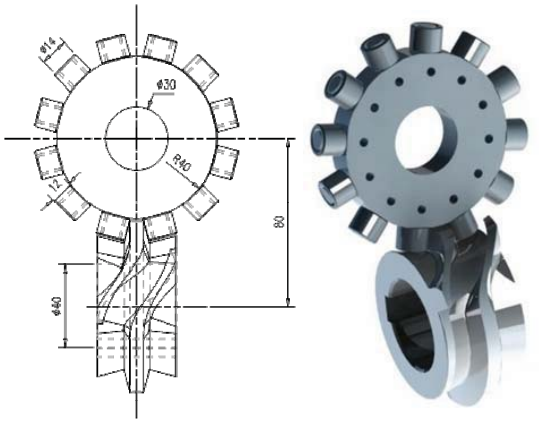

Fig. 7. The cam mechanism for the example.

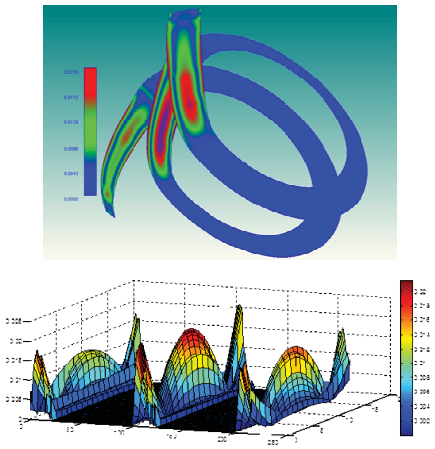

Fig. 8. Error distribution of Algorithm2.

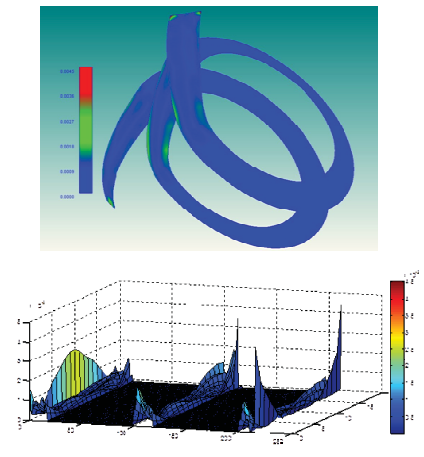

Fig. 9. Error distribution of LSQR.

machining accuracy requirements under most circumstances, thus make the next step superfluous. But in order to make our work more universal, we then apply the MINIMAX method described in chapter 3 to lower the error. A new tool trajectory is obtained. We then evaluate error, which is shown in Fig10:

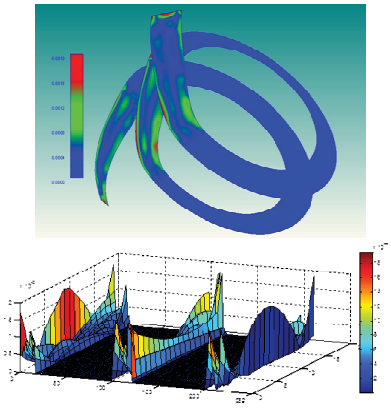

Fig. 10. Error distribution of MINIMAX.

As can be seen, the errors occur more in the indexing period, which broadly in line with the theatrical error distribution. It is also noticeable that the errors distribute evenly in the indexing period, which indicates there is still room for improvements. The comparison of optimization between different methods is illustrated in Table2.

TABLE II
MODAL ANALYSIS RESULT COMPARISON

Methods	Maximum error(microns)
Mid-point offset algorithm	54.3
Algorithm 2	21.5
LSQR	4.5
MINIMAX	1.9

Then the final result can be used to generate the tool path, which is shown in Fig11:

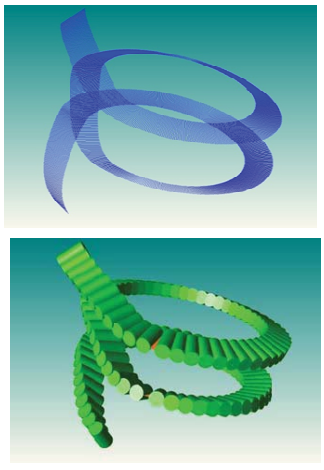

Fig. 11. Tool path for flank milling.

Now that the tool path is obtained, it's possible to generate the NC code for simulation and actual process. Fig12 shows the VERICUT simulation. The simulation indicates the process is interference free.

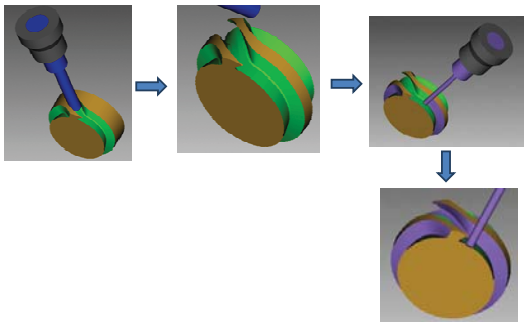

Fig. 12. VERICUT simulations.

V. CONCLUSION

The tool path planning method for 5-axis flank milling of a globoidal indexing cam is developed and validated. The discrete tool position is first optimized based on the instantaneous contact curve, and the flank milling tool path is finally globally optimized. Compared with the existing methods, the new method decreases the deviation between the cam profile and the cutter envelope surface. In the computational example, the deviation is less than 0.01mm that is an acceptable level. The method provides a high-efficiency and high-accuracy way to machine the globoidal indexing cam profile.

ACKNOWLEDGMENT

The authors gratefully acknowledge the financial support of the National Science and Technology Major Project (No. 2012ZX04010051), National Natural Science Foundation of China (No.51005155) and the National Basic Research Program of China (No. 2011CB706800).

REFERENCES

[1] H Y Chen and H Pottmann. Approximation by ruled surfaces. Journal of Computational and Applied Mathematics, 1999, 102(1): 143-156.
[2] Liu X W. Five-axis NC cylindrical milling of sculptured surfaces. Computer-Aided Design, 1995, 27(12): 887-894.
[3] Bohez E L J, Senadhera S D R, Pole K, Duflou J R, Tar T. A geometric modeling and five-axis machining algorithm for centrifugal impellers. Journal of Manufacturing Systems, 1997, 16(6): 422-436.
[4] Tsay D M, Her M J. Accurate 5-axis machining of twisted ruled surfaces. Trans. Of ASME, Journal of Manufacturing Science and Engineering, 2001, 123(4): 731-738
[5] Rubio W, Lagarrigue P, Dessein G, Pastor F. Calculation of tool paths for a torus mill on free-form surfaces on five-axis machines with detection and elimination of interference. The International Journal of Advanced Manufacturing Technology, 1998, 14(1): 13-20.
[6] Redonnet J M, Rubio W, Dessein G. Side milling of ruled surfaces: Optimum positioning of the milling cutter and calculation of interference. The International Journal of Advanced Manufacturing Technology, 1998, 14(7): 459-465.
[7] Bedi S, Mann S, Menzel C. Flank milling with flat end milling cutters. Computer-Aided Design, 2003, 35(3):293-300.
[8] Tsay D M, Her M J. Accurate 5-axis machining of twisted ruled surfaces. Trans. of ASME, Journal of Manufacturing Science and Engineering, 2001, 123(4): 731-738.

[9] Li C G, Bedi S, Mann S. Flank milling of ruled surface with conical tools - an optimization approach. The International Journal of Advanced Manufacturing Technology, 2006, 29(11-12): 1115-1124.
[10] Rong S L, Chen H S. Tool path generation and error control method for multi-axis nc machining of spatial cam. International Journal of Machine Tools and Manufacture, 1998, 38 (4) : 277-290
[11] Lee J N, Lee R S. Interference-free toolpath generation using enveloping element for five-axis machining of spatial cam. Journal of Materials Processing Technology, 2007, 187-188:10-13
[12] Rong S L, Jeng N L. New method of tool orientation determination by enveloping element for fiveaxis machining of spatial cam. International Journal of Production Research, 2002, 40 (10) , :2379-2398
[13] Grant B, Soni A H. Survey of cam manufacture methods. J Mech Des Trans ASME ,1979,101(3): 455-464
[14] Der M T, Hsien M W. A general approach to the determination of planar and spatial cam profiles. Journal of Mechanical Design, 1996,118(2):259-265.
[15] Tsay D M, Ho HC. Consideration of manufacturing parameters in the design of grooved globoidal cam indexing mechanisms. Proceedings of the Institution of Mechanical Engineers, Part C: Journal of Mechanical Engineering Science, 2001, 215 (1) : 95-103.
[16] Kong M, Hu Z H, Li H, et al. Cutter Location Optimization Algorithm for One-side NC Machining of Globoidal Cams Based on Equidistant Surfaces. Chinese Journal of Mechanical engineering. 2008, 44(11):277-282.